

## Electronic supporting information for the inside-out supercapacitor: induced charge storage in reduced graphene oxide

Samuel T. Martin<sup>a,b</sup>, Abozar Akbari<sup>a</sup>, Parama Chakraborty Banerjee<sup>a</sup>, Adrian Neild<sup>b</sup>, Mainak

Majumder<sup>a\*</sup>

### Table of Contents

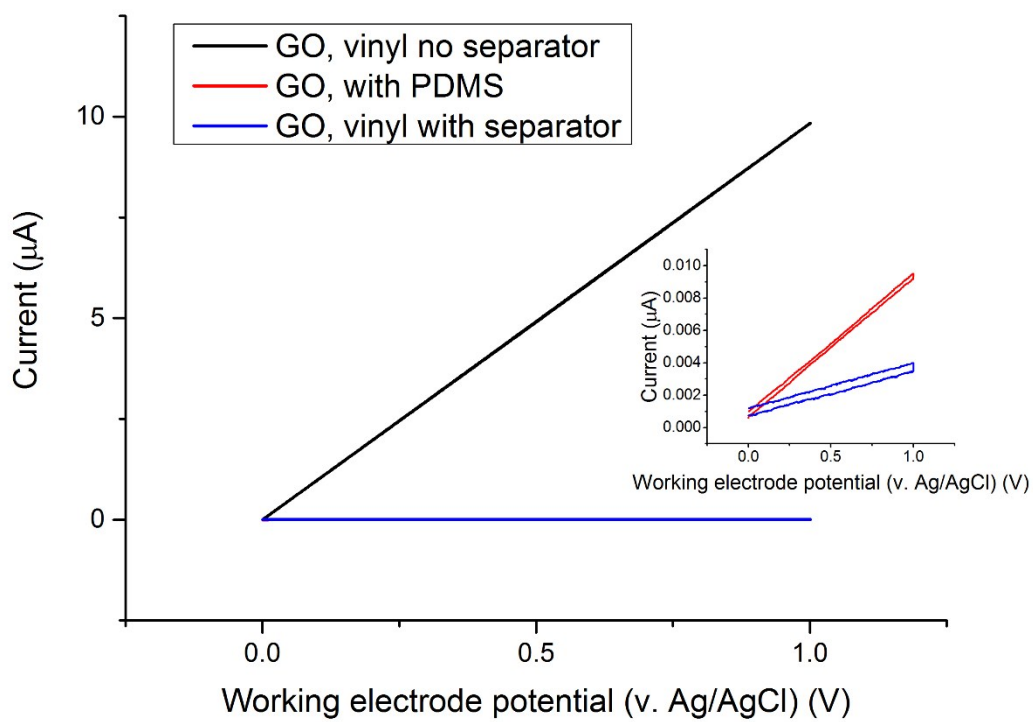
Role of the PDMS Separator .....	2
Varying the conductivity of reduced graphene oxide.....	5
Gold control inside out supercapacitor .....	7
Electrochemical calculations .....	8
Additional electrochemical characterization .....	10
Role of the vinyl seal.....	12

---

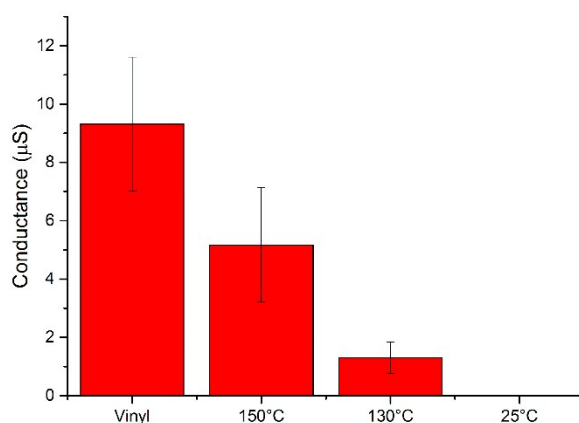
<sup>a</sup> *Nanoscale Science and Engineering Laboratory (NSEL), Department of Mechanical and Aerospace Engineering, Monash University Clayton, VIC-3800 Australia*

<sup>b</sup> *Laboratory for Microsystems (LMS), Department of Mechanical and Aerospace Engineering, Monash University Clayton, VIC-3800 Australia*

## Role of the PDMS Separator



*Supplementary figure 1- Cyclic voltammetry plot for 3 different graphene oxide (GO) based device designs. GO samples with no separator permit an unimpeded path for ion to travel through the interlayer spacing of the GO. GO devices where PDMS is used to penetrate into the microstructure of the film and block it exhibit radically reduced ionic conductance. These tests were performed at a scan rate of 1 mV/s in a 1M  $\text{Na}_2\text{SO}_4$  electrolyte.*



*Supplementary figure 2 - The conductance of a series of devices, sealed in different manners, one with a vinyl seal, three with PDMS seals cured at different temperatures (150 °C 130 °C and 25 °C) was monitored for 20 hours in 1 mM NaCl electrolyte. The 25 °C sample had an average conductance of 9 nS.*

PDMS cures more swiftly as temperature increases. GO devices were fabricated to test the effect of curing temperature on the resultant ionic conductance. The vinyl devices used in this control experiment have the same fabrication as described in figure 2 of the main text, except there is no slot present for PDMS to be cast into. This allows ions to move unimpeded parallel to the hydrophilic GO sheets from one reservoir to the other as described in Raidongia et al.<sup>1</sup> The PDMS based devices take a GO film on a glass substrate and buries the film in freshly prepared PDMS. This is then cured in the oven at various temperatures changing the diffusivity of the polymer, its curing time and its viscosity. Once cured the film is cut to length (14 mm) and reservoirs are attached using epoxy.

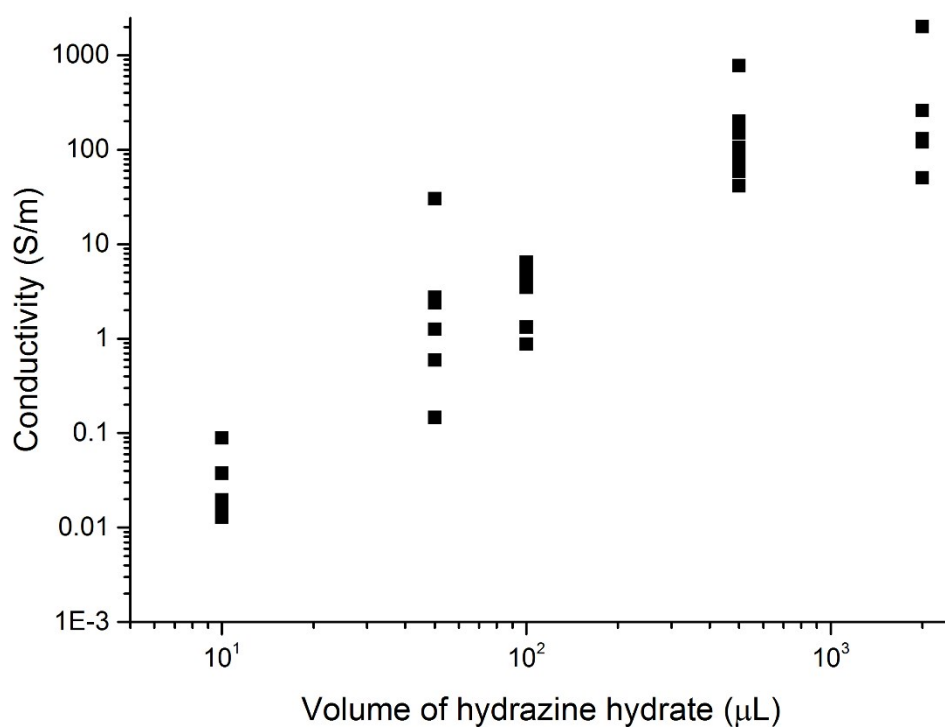
There's almost a 2-fold loss in conductance from the vinyl case to the PDMS cured at 150 °C, which is listed to cure in 5 minutes. From this there are two possible conclusions – the vinyl seal leaks or the PDMS penetrates rapidly into the film (these films are quite thin it should be mentioned, ~2 μm). If there is a leak it is uniform across all samples tested as the uncertainty doesn't really change between the PDMS case and the vinyl, which is somewhat unexpected in the case where the vinyl seal is leaking. When the temperature is decreased to 130 °C there is almost a 5-fold loss in

conductance from 150 °C despite only a 5 minute increase in curing time. This points to the fact that for these thin film the PDMS very rapidly penetrates and blocks the nanochannels of these devices.

The GO with PDMS device in Supplementary figure 1 was fabricated in the same manner as described in PDMS penetration testing section above. Once the pattern was formed 3 different designs were produced- those completely buried in PDMS, those with slots cut in the vinyl for PDMS penetration and devices with a vinyl seal and no PDMS. The PDMS was set over 24 hours allowing it to penetrate into the film.

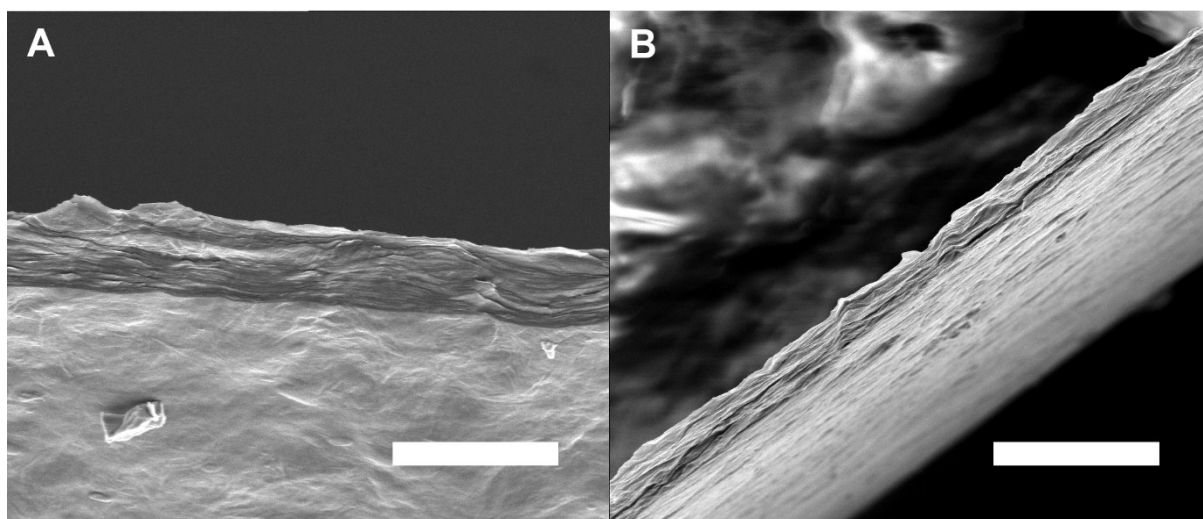
As can be seen in Supplementary figure 1, the device with no PDMS infiltration (one with a simple vinyl seal) has significantly higher ionic conductivity. The devices entirely buried in PDMS and one with a separator slot performed similarly with conductivities in the nS range. This suggests clearly that the separator is reducing ionic conduction in the material.

## Varying the conductivity of reduced graphene oxide



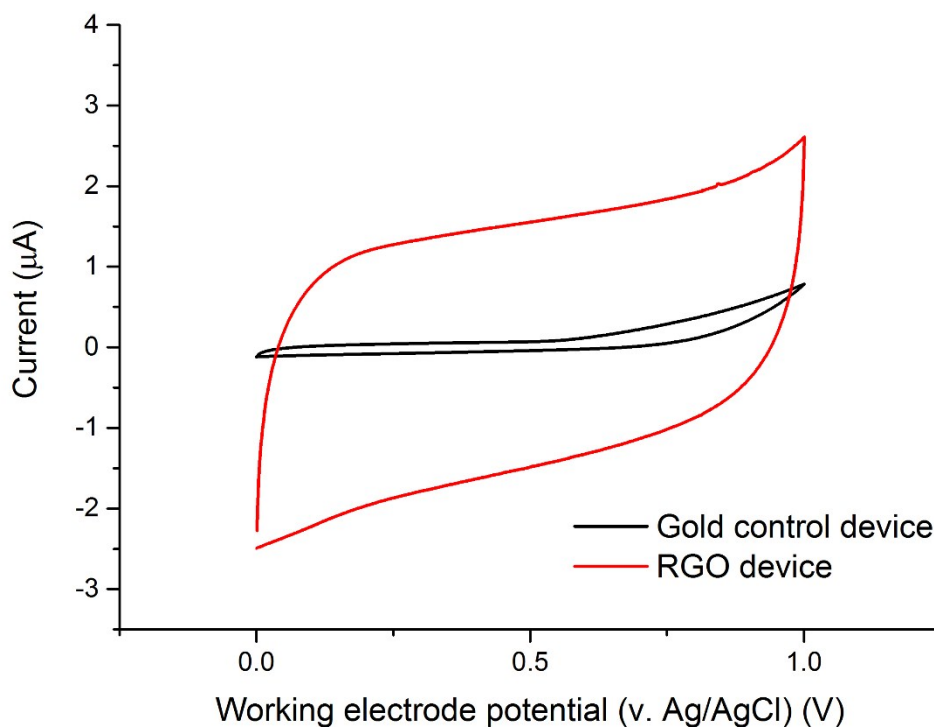
*Supplementary figure 3 – Various volumes of hydrazine were used to vary the level of reduction in the graphene oxide films. The conductivities here are calculated using the reduced sample's height measured using an optical profilometer.*

In order to vary the conductivity, samples were exposed to different quantities of hydrazine vapour as shown in Supplementary figure 3. The objective of this was to create a variety of samples with different conductivities to demonstrate that the resultant electrical properties were of key importance and not the exact quantity of reducing agent used.



*Supplementary figure 4 – a) a cross section of a graphene oxide film illustrating continuous film structure, b) a film sample exposed to 30  $\mu\text{L}$  of hydrazine hydrate, exfoliation has occurred due to the development of gas during reduction indicated by the presence of voids in the film structure. Scale bar in both figures is 10  $\mu\text{m}$ .*

## Gold control inside out supercapacitor



*Supplementary figure 5 – cyclic voltammograms of a typical RGO inside-out supercapacitor and a gold coated microscope slide with reservoirs adhered to its surface at a scan rate of 1 mV/s in 1M Na<sub>2</sub>SO<sub>4</sub> electrolyte.*

The gold device was prepared by sputtering a thin layer of gold onto a microscope slide. Reservoirs were then bonded onto the gold directly at two places on the slide and filled with electrolyte. The area of gold exposed to the electrolyte in each reservoir was 8 mm x 8 mm. The capacitance of the gold based device was small in comparison to the RGO device's. This is attributed to the difference in exposed specific surface area of the two materials. Both devices demonstrate induced double-layer charge storage and show the generality of the mechanism described here.

## Electrochemical calculations

The capacitance of a device was calculated using CV data at a given scan rate using, (calculations follow those used in Lobo et al.)<sup>2</sup>

$$C = \frac{1}{\nu \Delta \varphi} \int_0^1 i(\varphi) d\varphi, \text{ for } i > 0 \quad (1)$$

where  $\Delta \varphi$  is the applied potential window,  $\nu$  is the scan rate,  $i$  is the current and  $\varphi$  is the voltage.

This integral was calculated for the 5<sup>th</sup> cycle. To calculate the specific capacitance the capacitance value was divided by the volume of the work surface (6 mm × 14 mm × thickness).

Capacitance from GCPL data was calculated using

$$C = \frac{i}{-\frac{d\varphi}{dt}}, \quad (2)$$

where the derivative of  $\varphi$  is the gradient of the discharge curve.

Specific capacitance was calculated by

$$C_{sp} = \frac{C}{V}, \quad (3)$$

where  $V$  is the volume of the work surface. Power was calculated from the cyclic voltammetry data by

$$P = \int_0^1 i(\varphi) d\varphi, \text{ for } i > 0. \quad (4)$$

Power density was calculated using

$$\rho = \frac{P}{V}. \quad (5)$$

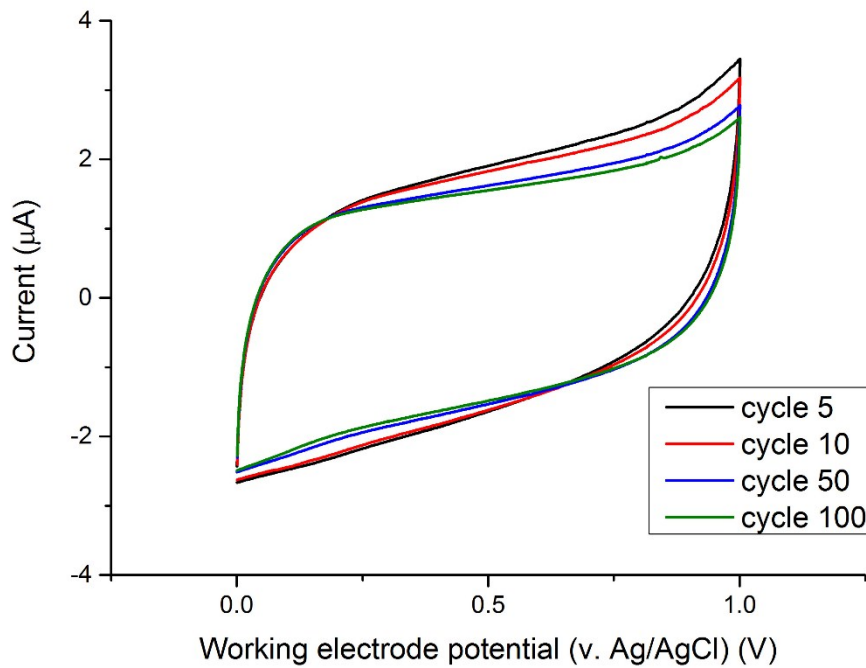


Areal capacitance was calculated using

$$C_{Areal} = \frac{C}{2A_{int}}, \quad (6)$$

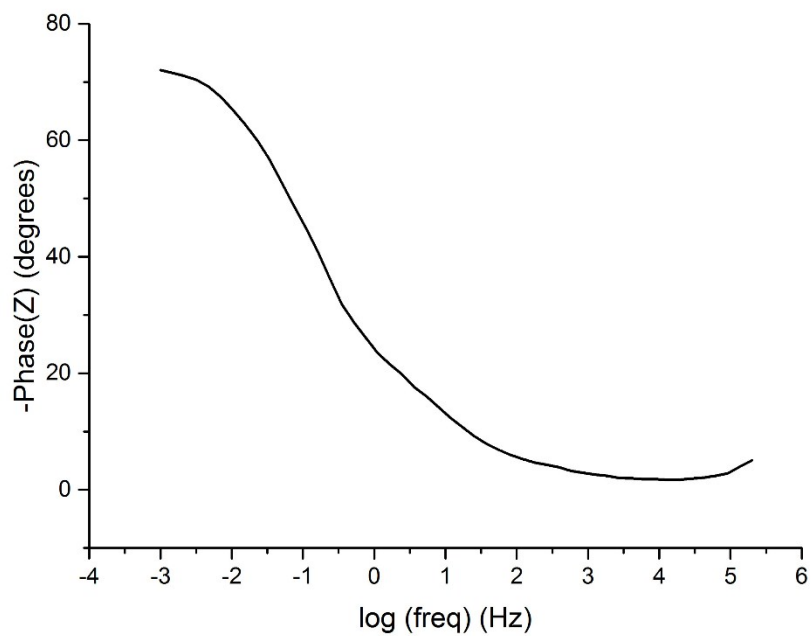
where  $A_{int}$  is the cross sectional area of the work surface.

## Additional electrochemical characterization

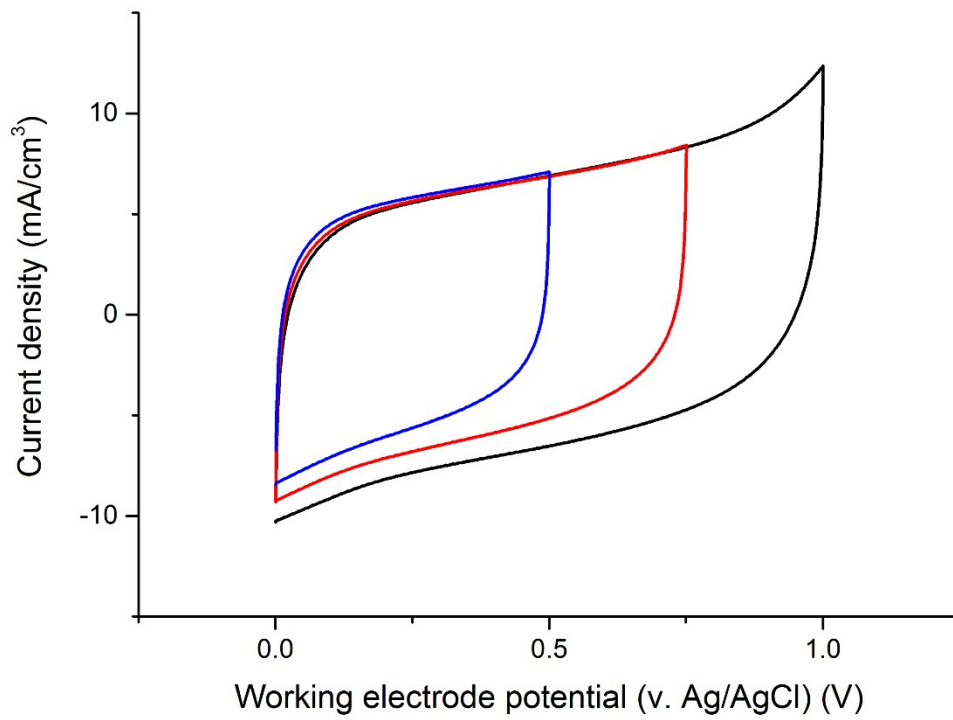


Supplementary figure 6 –Cyclic voltammograms for a 2.3 μm thick device scanned at 1 mV/s for 100 cycles in 1 M Na<sub>2</sub>SO<sub>4</sub>.

There is no significant change to the shape of the curve indicating the absence of faradaic reactions.



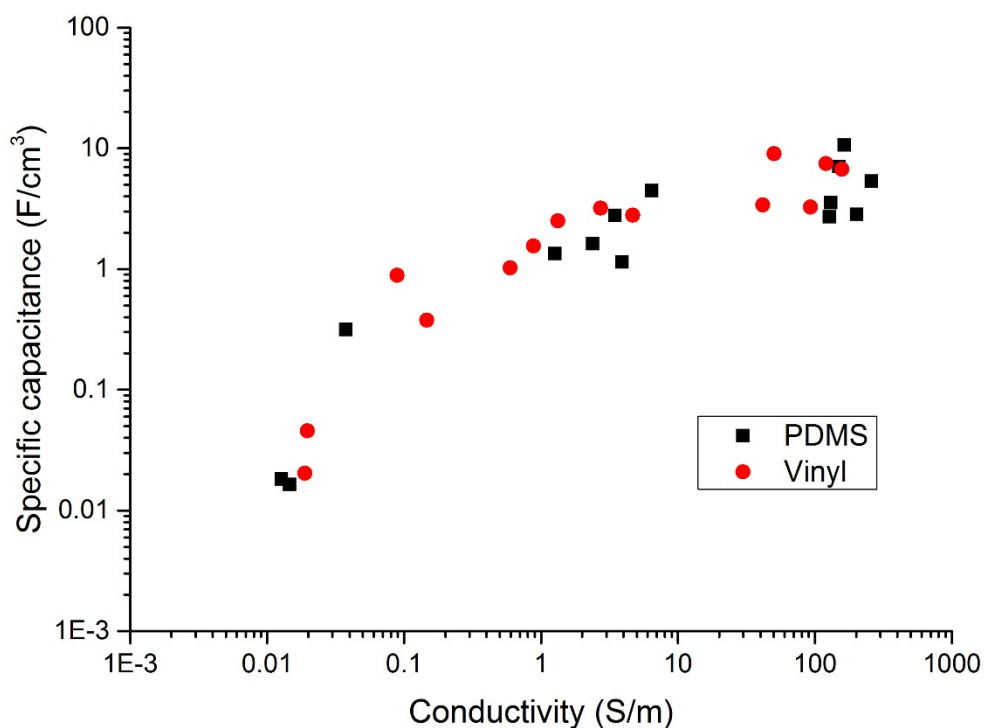
Supplementary figure 7 – A typical Bode phase plot for a 1 μm thick inside out supercapacitor.



*Supplementary figure 8 – Cyclic voltammograms for a 1  $\mu\text{m}$  thick device cycled at several different voltage ranges, in all cases the scan rate was 1 mV/s in 1 M  $\text{Na}_2\text{SO}_4$  electrolyte.*

## Role of the vinyl seal

Understandably the question must arise as to the efficacy of this vinyl seal in this concentrated salt solution. In this first experiment (Figure 3 and Supplementary figure 9) two different designs were used- a vinyl seal with a slot for the PDMS separator and a design that was purely PDMS with no vinyl. As it is known from previous experiments that PDMS will penetrate into GO and radically alter its ionic conductivity (Supplementary figure 1) this would suggest that no electrolyte penetrates into the RGO as the PDMS penetrates into the film and is given 24 hours at 25 °C to do so. According to Supplementary figure 1 this increases ionic resistance by around 3 orders of magnitude. It follows that if the electrolyte were to wet the entire vinyl covered film volume and/or form a thin wetting layer between the vinyl and the RGO then the vinyl case would have significantly more exposed area (as the current area exposed is  $\sim 6000 \mu\text{m}^2$ ) and thus higher capacitance. It is arguable that the vinyl design slightly outperforms the PDMS one (Supplementary figure 9) which we attribute to the PDMS preventing electrolyte entering the porous work surface at the exposed ends which one might expect given the results in Supplementary figure 1 and not as a result of the vinyl seal exposing more area than proposed. However it is quite clear that regardless of the method the performance depends far more strongly on the conductivity of the work surface than the exact nature of the separator and device design.



Supplementary figure 9 – Specific capacitances at a scan rate of 1 mV/s in a 1M Na<sub>2</sub>SO<sub>4</sub> electrolyte for the two different device fabrications – one with a vinyl seal and PDMS separator and one entirely coated in PDMS.

## References

1. Raidongia K, Huang J. Nanofluidic Ion Transport through Reconstructed Layered Materials. *J Am Chem Soc* **134**, 16528-16531 (2012).
2. Lobo DE, Banerjee PC, Easton CD, Majumder M. Miniaturized Supercapacitors: Focused Ion Beam Reduced Graphene Oxide Supercapacitors with Enhanced Performance Metrics. *Advanced Energy Materials* **5**, (2015).